Seismic imaging and modelling of the lithosphere of SW-Iberia

I. Flecha [a,*], I. Palomeras [a,1], R. Carbonell [a,1], F. Simancas [b,2], P. Ayarza [c,3],
J. Matas [d,4], F. González-Lodeiro [b,2], A. Pérez-Estaún [a,1]

[a] Departament de Geofísica i Tectònica, Institut de Ciències de la Terra "Jaume, Almera"-CSIC, C/ Lluis Solé i Sabaris s/n, 08028 Barcelona, Spain
[b] Departamento de Geodinámica, Universidad de Granada, Av. Fuentenueva, s/n, 18071 Granada, Spain
[c] Departamento de Geología, Universidad de Salamanca, 37008 Salamanca, Spain
[d] Instituto Geológico Minero de España, C/ Ríos Rosas, 23, 28003 Madrid, Spain

ARTICLE INFO

ABSTRACT

Data from a closely spaced wide-angle transect has been used to study the middle-to-lower crust and the Moho in SW-Iberia. A low-fold wide-angle stack image reveals a highly heterogeneous seismic signature at lower-crustal levels changing laterally along the profile. The lower crust features an irregular distribution of the reflectivity that can be explained by a heterogeneous distribution of physical properties. The Moho discontinuity also features a high variability in its seismic character that correlates with the different tectonic terranes in the area. A 2D finite difference code was used for solving the elastic wave equation and to provide synthetic wide-angle shots. Relatively simple layer cake model derived from conventional refraction interpretation generates the main events of the shot records. However, these models cannot account for the lateral variability of the seismic signature. In order to obtain more realistic simulations, the velocity model was modified introducing stochastic lensing at different levels within the crust. The resulting average velocity models include a high velocity layer at mid-crustal depth, a highly reflective lower crust and a relatively thin horizontal Moho. This heterogeneous model can be achieved by lensing within the crust, a layered mafic intrusion and a strongly laminated lower crust and Moho.

1. Introduction

The lower crust and the Moho are major issues in deep geophysical prospecting. The knowledge about these parts of the Earth crust is limited because of the lack of direct information at this level of the lithosphere. Nevertheless, some outcrops have been identified as corresponding to lower crust materials. Good examples are the Cabo Ortegal complex (Peucat et al., 1990; Galán and Marcos, 1997; Martínez-Catalán et al., 1997; Santos-Zalduegui et al., 1997) and the Ivrea Zone (North Italy; Rutter et al., 1999). In both these cases several studies have been carried out and their crustal composition and the distribution of physical properties are well known (Holliger and Levander, 1992; Holliger et al., 1993; Levander et al., 1994b). Since the lower continental crust is not accessible for direct investigation, the main source of information about its physical properties and composition comes from indirect methods such as deep seismic

surveys. Seismic vertical incidence reflection profiles provide images where geometric information about the crustal structure can be obtained and wide-angle experiments provide data about physical properties (P-wave and S-wave velocities). These physical properties can then be inverted to composition by comparing with lithologies measured in laboratories. Results from these methodologies and its correct interpretation are probably the best tools available in order to understand geological processes at lithospheric scale.

Since the early 1990's, a large research effort has been devoted to studying SW-Iberia (e.g., the EUROPROBE (Ribeiro et al., 1996) and GEODE (Blundel et al., 2005) international programmes). One of the main objectives of these programmes was the acquisition of the high resolution normal incidence deep seismic reflection transect IBERSEIS (Simancas et al., 2003; Carbonell et al., 2004). The presence of large mineral deposits in the southwestern part of the Iberian Península, within the Pyrite Belt, and surrounding areas, suggests that the crust features particular physical properties and that it underwent a singular tectonic evolution. Therefore, extensive geological and geophysical research has been undertaken in the area.

The project IBERSEIS-WA consisted in two wide-angle transects acquired in SW-Iberia. A wide-angle stack of one of the wide-angle dataset (transect B, Fig. 1) is presented in this study. The specific target of this research is the nature of the lower crust and Moho. Furthermore, synthetic seismic modelling is carried out in order to explain the
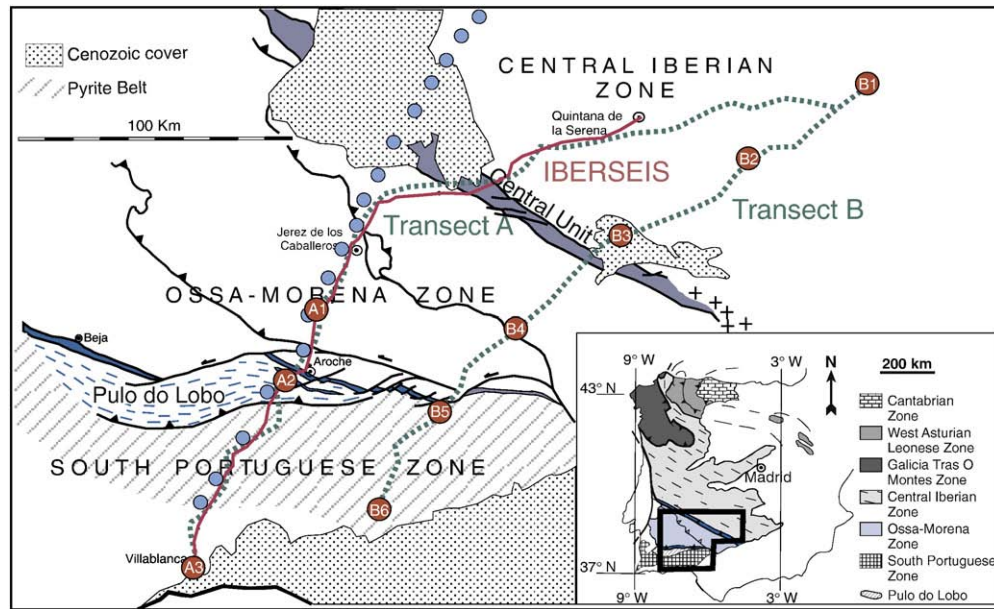
Fig. 1. Location map of the study area. The three tectonic terranes and its contacts are indicated. PL indicates Pulo du Lobo unit and CU indicates Central Unit. Dashed green lines indicate the wide-angle profiles and the red circles the shot points. Other surveys in the area are also shown: IBERSEIS deep seismic reflection transect (red line) and a magnetotelluric survey (blue circles). Data used in this work correspond to the eastern wide-angle profile, transect B. Modified from Palomeras et al. (2009).

particular characteristics of the shot-gathers and of the wide-angle stack. The main objective of the present study is to provide reliable images and geometrical models that can account for the seismic signature observed in the wide-angle dataset.

2. Geological and geophysical setting

The study area is located in the SW of the Iberian Massif, it is known to be an orogenic belt of Variscan age developed by the collision of a number of continental blocks. The area involves three tectonic terranes: South-Portuguese Zone (SPZ), Ossa-Morena Zone (OMZ), and Central-Iberian Zone (CIZ) (Fig. 1). These terranes are considered to be fragments of a Late Proterozoic mega continent which broke up in Early Paleozoic. The boundaries that limit these terranes have been interpreted as suture zones and include units of high-pressure rocks (Simancas et al., 2001).

The SPZ, which includes the Iberian Pyrite Belt, features within the upper crust a south-west vergent thrust system. The northern boundary of this zone is indicated by a series of slices of high-pressure rocks, the Beja Acebuches complex located to the north of the Pulo do Lobo Unit (Simancas et al., 2001, 2003). The surface outcrops of this contact (SPZ/OMZ) reveal fabrics that are indicative of a strike-slip component of the collision (i.e. transpression). The OMZ is mostly consistent of synforms and antiforms. This zone is limited to the north by the Central Unit (CU), and outcroping fault bounded wedge of metamorphic rocks with structural fabrics revealing strike-slip movement. Farther to the north, the CIZ features normal faults that cut recumbent folds resulting in basins of carboniferous age (Simancas et al., 2003). These structures suggest a domino-like extensional system. The surface evidences for strike-slip movement indicate that the orogen went through a strong transpression regime during its development.

A detailed geological study of the area can be found in Simancas et al. (2001) and references therein. The contribution of the IBERSEIS deep seismic reflection transect, acquired in the same area, can be found in Simancas et al. (2003) and in Carbonell et al. (2004). Finally, the crustal model derived by traveltime interpretation of the wide-

angle dataset and the geologic implications on the nature of the lower crust are discussed in detail by Palomeras et al. (2009). A relevant feature within the IBERSEIS deep seismic reflection transect is the IRB (Iberian Reflective Body) reflection, a 140 km long and 4 km thick high-amplitude reflective body which has been proposed to be related to the high concentrations of mineral deposits present mainly in the OMZ (Casquet et al., 2001; Tornos et al., 2001; Carbonell et al., 2004). This anomalous body was also reported as a high velocity zone in the refraction modelling with an extended distribution over the southern part of the Iberian Variscan Belt (Palomeras et al., 2009).

3. Wide-angle data: low-fold stack

The main objective of the low-fold wide-angle stack is to obtain a simplified structural image of the deep crust to the south-east of the IBERSEIS normal incidence transects. To the northwest, the crustal structure is well constrained by the IBERSEIS normal incidence transect.

The wide-angle seismic reflection data has station spacing of 150 m on average, making it suitable for generating a low-fold wide-angle stack. Following the conventional normal incidence processing, we used the acquisition geometry to define the CMP's. Then, following Carbonell et al. (1998, 2002), we designed a hyperbolic time shift to flatten the lower crust and the Moho reflections so that these events stack constructively within a CMP. Conventional NMO can be applied to wide-angle seismic reflection data, although this is not the optimum correction as it generates large artifacts when deep events and large offsets are considered. Therefore a hyperbolic time shift was preferred. The shot records were processed to emphasize the deep reflectivity. The data was Butterworth band-pass filtered (from 1 Hz to 35 Hz) and a time-dependent gain was applied to enhance the signal from the Moho. Also, the shot-gathers were displayed using an estimate of the seismic energy (Fig. 2). This was achieved by calculating the envelope using the Hilbert transform. Since we are interested in deep events, the first arrivals were muted to avoid its influence for displaying purposes. After this pre-processing the Moho can be displayed as a flat 1–2 second thick event (Fig. 2). As in the raw
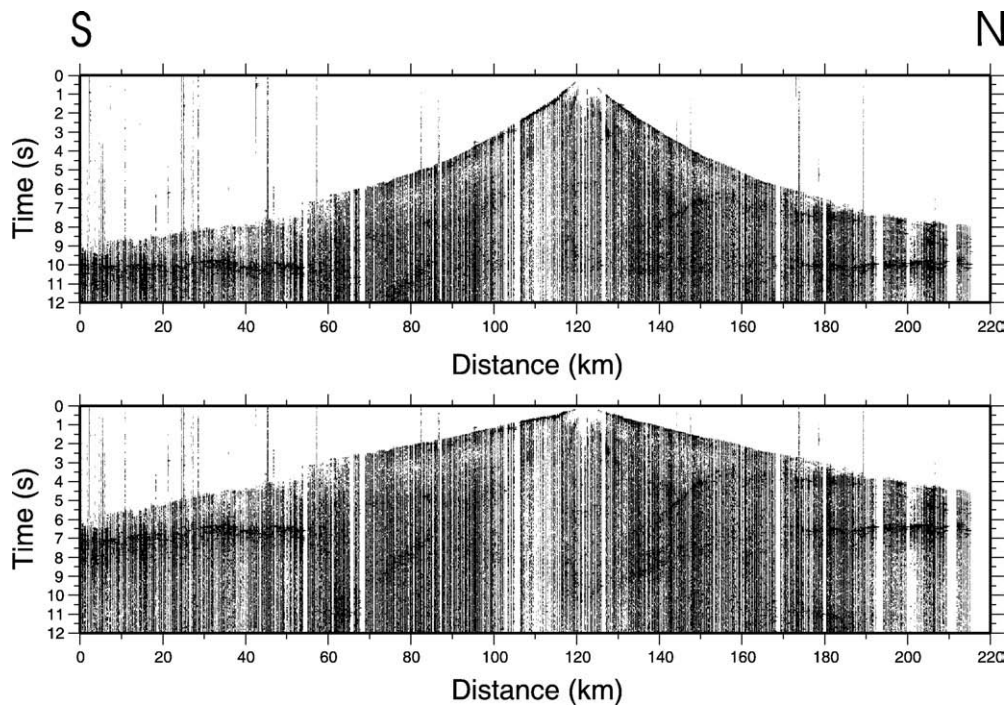
Fig. 2. Wide-angle shot-gather B3 after a hyperbolic shift using as a crustal average velocity 6.0 km/s (top) and after a linear reduction using 8.0 km/s as a reduction velocity.

data, some other coherent reflectors can be observed in the data as reflective packages at lower-crustal levels, which may image the structure in this part of the crust. The geometry of the mid-to-lower crust and the Moho reflections can be considered approximately correct with the applied time shift. An average crustal velocity deduced from Palomeras et al. (2009) was used to design this time shift.

3.1. Data description

Data after applying the hyperbolic shift are presented in Fig. 3. Shot B6 images strong reflectivity in the lower crust (6.5 to 8.5 s twtt) between 20 and 70 km. The Moho in this shot is not well resolved at short offsets (<40 km), probably because it is masked by the high-amplitude reflectors in the lower crust. At long offsets (>40 km), the Moho is imaged as a thick reflective package that slips slightly to the north. In shot B5 the Moho is imaged as a thin weak reflector at normal incidence (10 s twtt) while to the north it becomes a thicker event. Some reflectivity can be observed in the lower crust, matching the strong reflectivity exhibited by this zone in the previous shot B6. At 5.5 s twtt and normal incidence there is a prominent event, but due to the hyperbolic shift applied to the data it is difficult to determine its real geometry. Shot B4 displays strong reflectivity at lower-crustal levels, including a prominent south-dipping event between 30 and 45 km and 7.5 and 8.5 s twtt. To the north, a broad band of reflectivity (10.5 s twtt) is associated with the Moho. Shot B3 reveals a very well-defined PmP phase at 10 s twtt that delineates an almost flat Moho. The seismic signature varies significantly along this shot-gather, decreasing in thickness and complexity from south to north. A south-dipping event can be observed in the middle crust between 130 and 140 km and 6.5 and 8.5 s twtt, and is interpreted to be related to a near vertical structure because it cannot be identified in other shot-gathers. Shot B2 exhibits a clear, thick reflective package at 10 s twtt that extends laterally between 80 and 140 km. This event displays a changing characteristic along the profile. At normal incidence, the Moho is weakly imaged for positive offsets (north). In shot B1 there is large amount of reflected energy between 170 and 180 km, associated with the Moho. It can be followed to the south although it becomes diffuse. In the last 50 km to the north, the lower crust is highly reflective. Some

of the events described previously are masked in the stacked image (Fig. 3) because there are reflectors that can only be imaged in single shot-gathers. However, the main features, especially the Moho, will be enhanced due by the constructive summation of seismic amplitudes. These are described below for each tectonic zone.

3.2. South Portuguese Zone (SPZ)

Within this area (0–40 km, Fig. 3) some relatively short reflectors can be observed at lower-crustal levels (between 7.5 and 8.5 s twtt). The Moho transition is identified as a thin weak reflection at 9.5 s in time (Fig. 3). Shots B5 and B6, reveal a simple event for the Moho which increases in thickness towards the east (Fig. 3). The lower crust reveals strong reflectivity that may be responsible for the back-scattered energy observed at 7–8 s twtt in the shot records. Thus, the seismic energy travelling through this structure has been noticeably decreased resulting in a weaker amplitude for deeper interfaces.

3.3. Ossa Morena Zone (OMZ)

In this part of the profile (40–110 km, Fig. 3) there are some prominent lower-crustal events in the southern part (40–60 km). To the north, this character changes and the lower crust becomes transparent. The Moho consists of a very reflective package at around 10 s twtt, with a variable thickness increasing from 1 s in the south to 2 s in the north. The change in the crust–mantle seismic signature would indicate a more complex structure compared with the SPZ.

3.4. Central Iberian Zone (CIZ)

In the second half of the profile (110–220 km, Fig. 3) the seismic energy appears as isolated packages around 10.5 s in depth. In the last part of the profile (190–210 km), some events are displayed in the lower crust at 7–8 s twtt.

4. 2D-modelling: from real data to synthetic simulations

In general, deep crust seismic data is often characterized by a high reflectivity compared to a relatively transparent upper crust (Martini
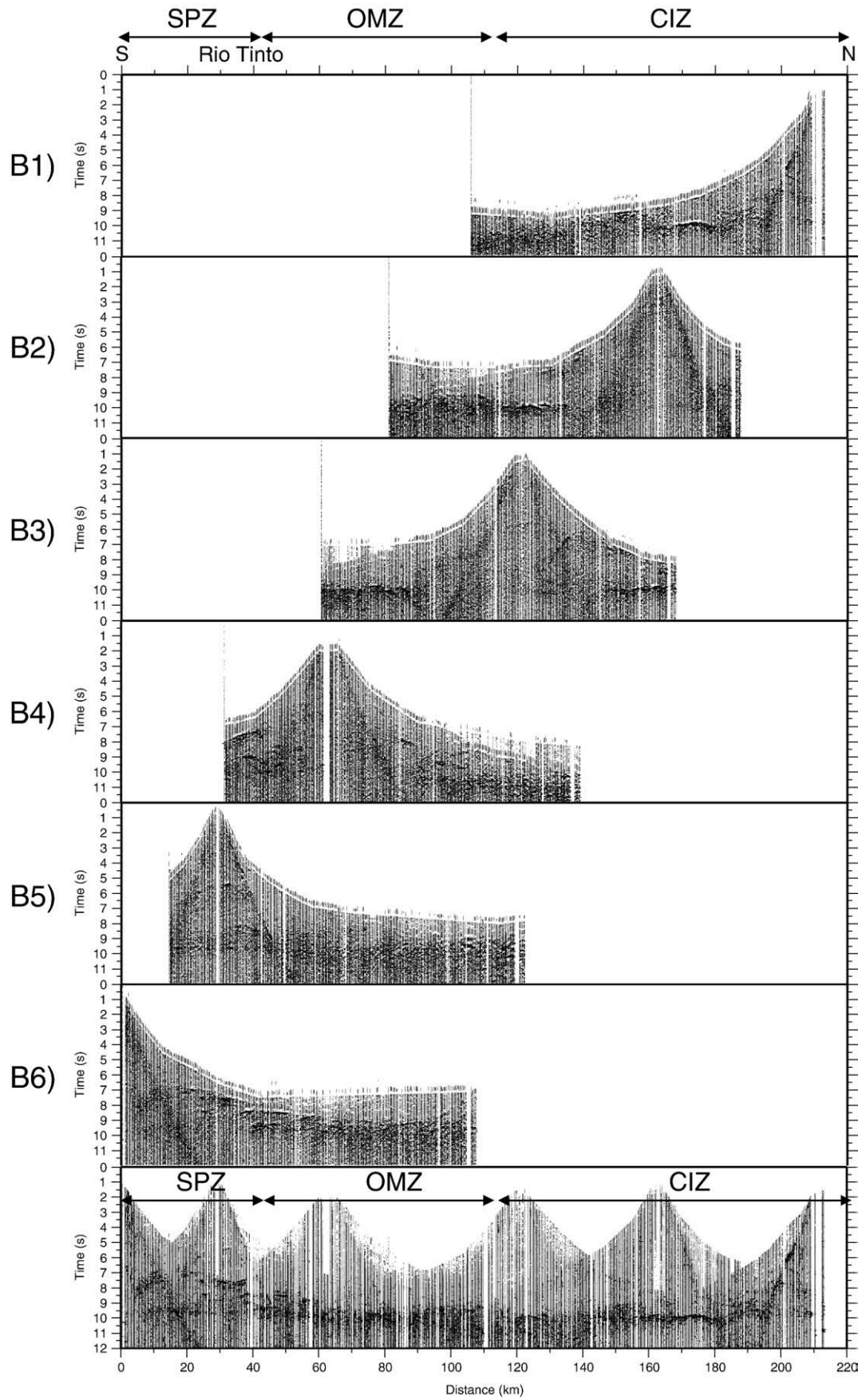
Fig. 3. From top to bottom: shot-gathers B6, B5, B4, B3, B2, B1 and stack. The shot-gathers are displayed in the CDP domain after applying a hyperbolic time shift. The three tectonic units are labelled as: SPZ (South Portuguese Zone), OMZ (Ossa Morena Zone) and CIZ (Central Iberian Zone).

et al., 2001). This reflectivity is normally composed of short, discontinuous reflections which usually appear in distinct packages confined to one or more parts of the crust (Holliger and Levander, 1992). It has been proposed that relatively small changes in composition and/or meta-morphic grade, may substantially affect the reflectivity of the lower crust (Holliger et al., 1993). Otherwise, observed reflection amplitudes are often larger than the ones predicted by the reflection coefficients based on crustal composition which can be explained by the result of constructive interference between individual reflection wavelets (Hurich and Smith-son, 1987). Reflection coefficients and reflection amplitudes are depen-dent upon the contrasts in acoustic impedance and not on bulk velocity (Deemer and Hurich, 1994), therefore a layered lower crust could be considered to justify these coefficients. This option would also account for reverberations in the data that cannot be explained by a single reflecting interface. The seismic signature featured by the acquired data can also be achieved by considering a lateral and vertical random velocity fluctuation (Gibson and Levander, 1988; Carbonell and Smithson, 1991). Isotropic random variations are consistent with models of lower-crustal petrologic processes, which may include igneous intrusions (Gibson and Levander, 1988). Hence, the most plausible scenario to satisfactorily describe the field data may consist of a random lamination or lensing coupled with random changes in rock properties. It has been shown that reflection seismic lines shot in the Variscan orogen display a strongly reflective lower crust characterized by numerous short horizontally embedded reflectors (Wenzel et al., 1987). Furthermore, field observations show that the crystalline rocks of the continental crust are often characterized by compositional variations at many scales (Hurich and Smithson, 1987) spanning at least seven orders of magnitude, from microfabrics ($\leq 10^{-3}$ m) to major crustal units ($\geq 10^4$ m) (Holliger et al., 1994).

Seismic theory establishes that Fresnel diameter is given by:

$$d \approx \sqrt{2z\lambda + \frac{\lambda^2}{4}} \qquad (1)$$

and is the smallest resolvable feature in unmigrated seismic data, delimiting the measure of lateral resolution. Hence, crustal features smaller than Fresnel diameters are not expected to be recovered as coherent seismic events. However, fine-scale velocity fluctuations can fundamentally change the character of signals from the crust (Levander et al., 1994a). Seismic modelling has demonstrated that spatial interference is important during the formation of the reflection wavefield. Interference may result from reflecting bodies smaller than the Fresnel zone (small body diffractors), therefore constructive interference can be equally as important as compositional variation for determining reflection amplitudes (Hurich and Smithson, 1987). All these considerations must be taken into account in any model able to reproduce the crustal seismic response.

4.1. Forward modelling

The seismic velocity model (Fig. 4) obtained by Palomeras et al. (2009) indicates a maximum crustal thickness of ~33 km with a Moho characterized by a flat topography. However, the most remarkable feature from the refraction modelling is the high velocities at middle-crust levels. Velocities of 6.8 km/s to 6.9 km/s define a 70 km long lens located at 17 km in depth in the southern part of the profile. Towards the north, slightly higher P-wave seismic velocities have been modelled and can go as shallow as 12 km in the northern end of the profile (Palomeras et al., 2009).

Considering the velocity model obtained by Palomeras et al. (2009), forward modelling has been carried out using a second order finite difference solver for the elastic wave equation which includes all primary and multiple reflections (Sochacki et al., 1987, 1991). In some cases, the lower crust reflectivity patterns have been successfully modelled by using one-dimensional reflectivity codes (Wenzel et al., 1987; Carbonell et al., 2002). However, in the present study there are a priori reasons to think that the lower crust is a laterally inhomogeneous media (Palomeras et al., 2009). The previous IBERSEIS normal incidence experiment and the wide-angle stack are also indicative of a laterally heterogeneous media, therefore a two dimensional approach was preferred because one-dimensional modelling of wide-angle data would only result in a laterally averaged interpretation.
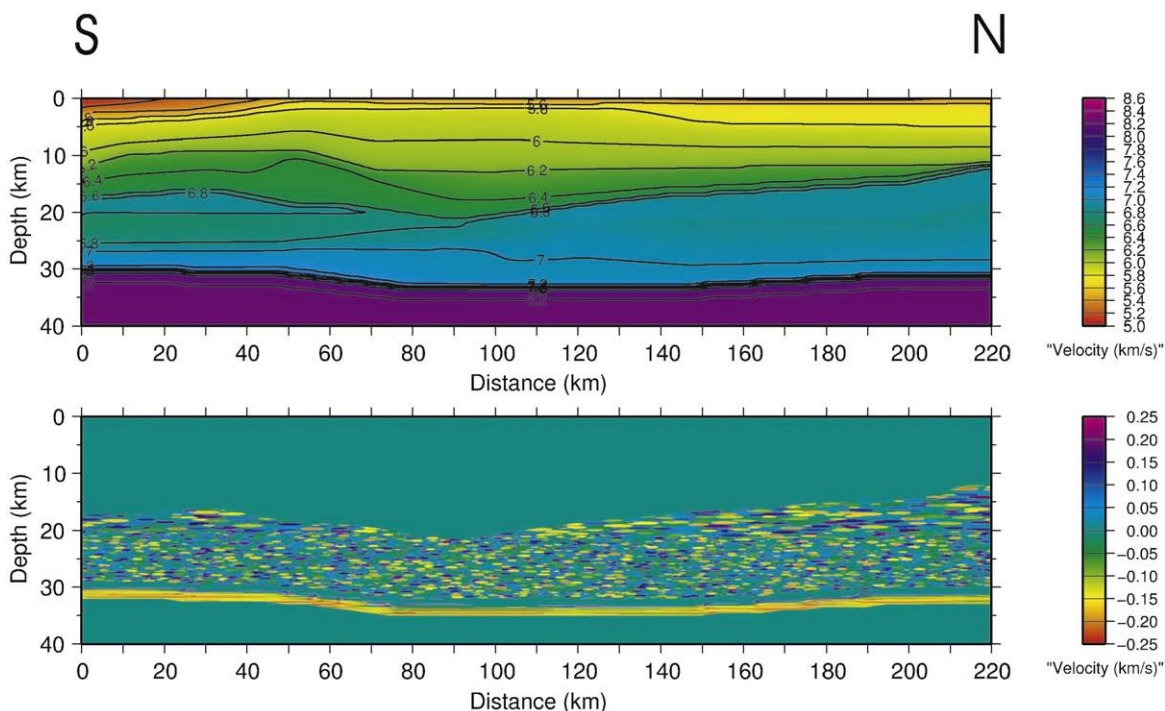

Fig. 4. Top: Velocity model obtained from refraction modelling (modified from Palomeras et al. (2009)). Bottom: Difference between refraction model and a modified velocity model to include the stochastic lensing representing mafic intrusions and lower crust as well as the layered structure of the Moho (bottom).

The P-wave velocity model derived from the refraction processing and interpretation was resampled using a 25×25 m grid which is appropriate for modelling crustal-scale seismic data. As the elastic approximation was used, also density and S-wave velocity were introduced as inputs in the code. The S-wave was calculated from the P-wave velocity using a V_p/V_s ratio of $\sqrt{3}$, and the density model was derived from V_p using the Christensen relation $\rho = 1.85 + 0.169V_p$ (Christensen and Mooney, 1995). In the resulting shot-gathers, traces were simulated in the same locations as the real receivers, the trace length was 30 s and the sampling rate was chosen to be 2 ms. With these synthetic simulations the main events in the real wide-angle shot-gathers were qualitatively well recovered (Figs. 5 and 6) because dominant reflections/refractions correlate with the boundaries of major lithological units. However, in the original shot-gathers, some events feature a complex signature consisting in a thick reflective package instead of an isolated event. The presence of these less well-defined events indicates that layering/lensing may be contributing to the seismic response. This fact forced us to consider a more sophisticated approach to model the lower crust and the mid-crustal high velocity areas.

4.2. Stochastic layering

It is well known that refraction techniques provide information about velocity, but depending on the depth (Fresnel zones), the accuracy is insufficient to assess the fine structure of the crust. Using these methodologies, major structures and discontinuities can be resolved within the crust. For the middle and the lower crust, the refraction velocity model represents an averaged background model which can fit correctly the picked traveltimes but, at small scale, it is unable to reproduce heterogeneities that feature the crustal velocity distribution. Probably the lower crust exhibits lateral heterogeneities that cannot be correctly modelled by using conventional ray tracing methods. In the recorded shot-gathers some of the phases consist of a thick reflective package instead of isolated events. This seismic signature cannot be reproduced with a simple smoothed layered model. In order to recover the observed reflectivity patterns some modifications were carried out in the velocity models to include some degree of complexity able to reproduce the seismic response recorded in the field data.

In SW-Iberia there are no outcrops of lower-crustal rocks where geological information can be obtained in order to characterize a realistic geometry and composition of this part of the crust. However, there is no seismological evidence that, apart from pressure and temperature, in situ conditions of the lower crust differ from those of its surface exposures (Wenzel et al., 1987). As the profile was acquired across Variscan terranes, we took physical properties (velocities) and geometrical information for the synthetic simulations from studies of the Variscan lower crust of Wenzel et al. (1987), Holliger and Levander (1992), Holliger et al. (1994). For the mafic intrusion, typical parameters
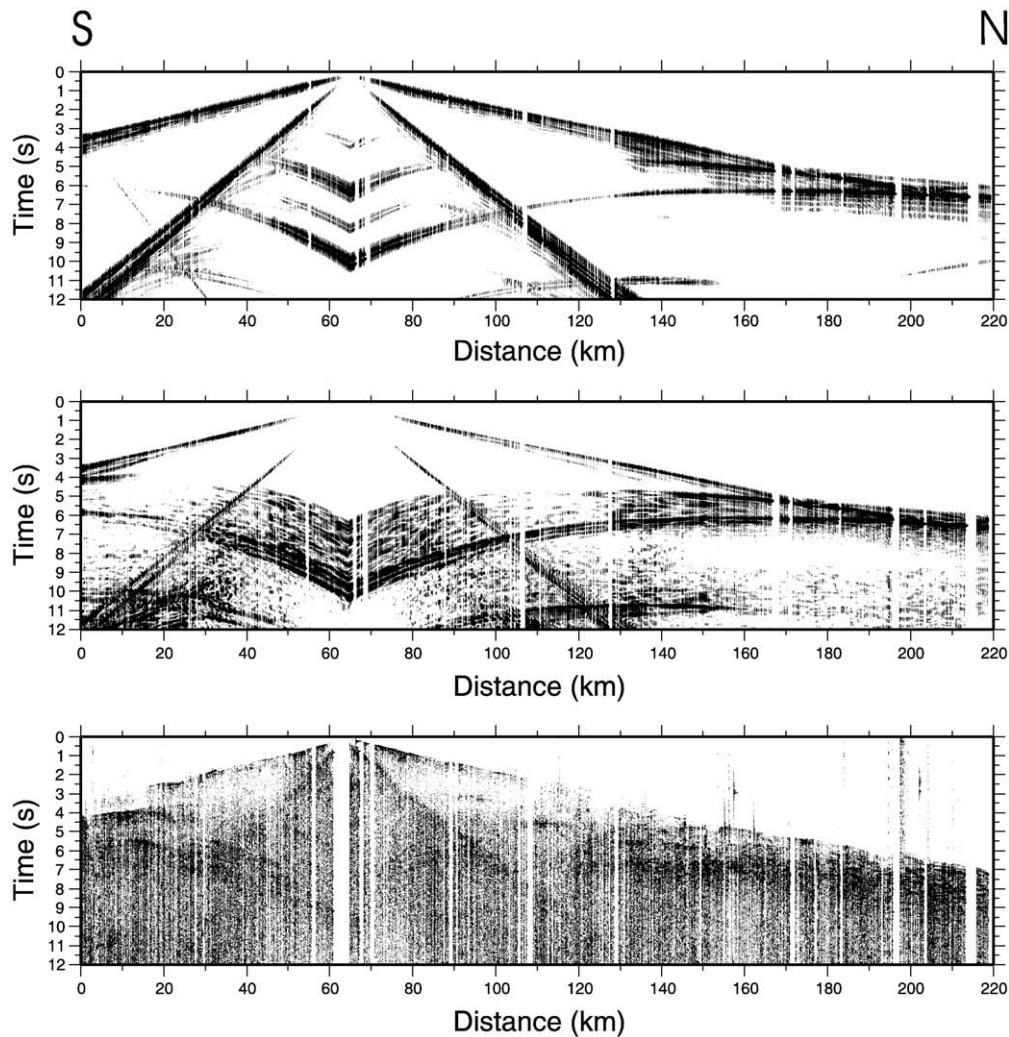

Fig. 5. Shot B4. Top: Synthetic seismic record section generated by using the homogeneous refraction velocity model. Middle: Synthetic seismic record section generated by using the heterogeneous velocity model consisting of a background velocity model which corresponds to the refraction model and the inclusion of the heterogeneities (high velocity lenses). Bottom: Real data. The synthetic sections were generated using a 2D elastic finite difference scheme.
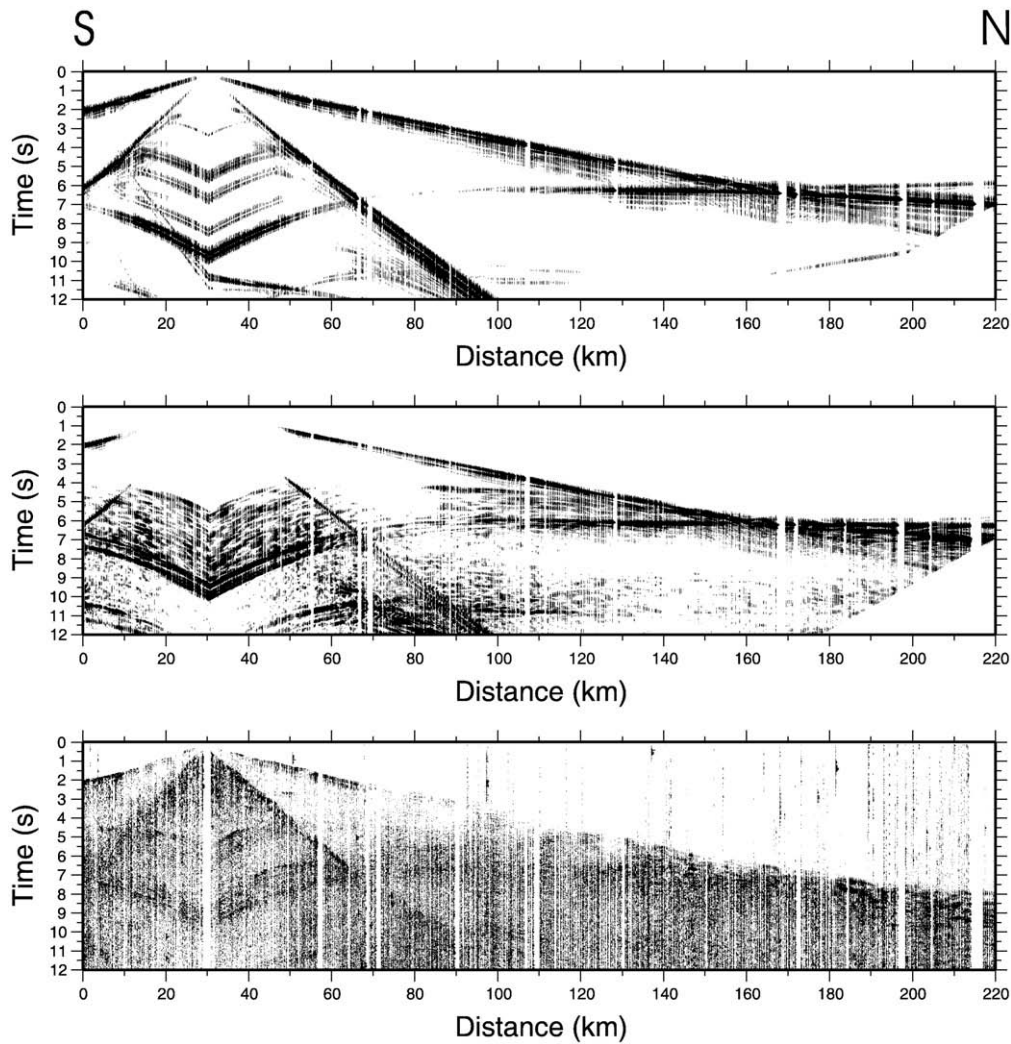
Fig. 6. Shot B5. Top, middle and bottom images correspond to the same than in Fig. 5 for the shot B4.

were taken from Deemer and Hurich (1994). At a small scale, a deterministic description of structures is unreasonable (Holliger et al., 1994), therefore a stochastic approach was applied. A new velocity model was built based on the one obtained by seismic refraction as starting point. The upper and middle crust were left unchanged whereas the high velocity layer, the lower crust and the Moho discontinuity were modified introducing lensing at different scales. The lensing was achieved by considering a set of ellipses randomly distributed along the high velocity layer and the lower crust. The center of every ellipse was chosen using a random function. The parameters defining the ellipse (semimajor axis and semiminor axis) were chosen arbitrarily ranging between a minimum and a maximum correlation length in both axes. Finally, the velocity for every ellipse was also randomly chosen considering a maximum variation of the aleatory measurements within

Table 1
Values used to modify the refraction velocity model in order to obtain a random layered model for the mafic intrusion, the lower crust and the Moho discontinuity.

	Mafic Intrusion	Lower crust	Moho
Bulk velocity (km/s)	6.7	7.1	7.85
Velocity variation (km/s)	±0.2	±0.2	±0.25
X dimension (km)	1–3	0.4–1.2	5–25
Z dimension (km)	0.1–0.2	0.025–0.2	0.025–0.1

Values were approximated from the literature (Wenzel et al., 1987; Holliger and Levander, 1992; Deemer and Hurich, 1994; Holliger et al., 1994).

the range of possible values of velocities for lithologies possible at this depth. The limit values for dimensions and velocities are summarized in Table 1. Both velocity models (with and without stochastic layering) are displayed in Fig. 4.

The Moho can be identified because it features a sharp change in velocity. Classically, the Moho has been considered as a velocity discontinuity with some lateral continuity. Most authors tend to model this as a simple interface, a line avoiding any additional structure except by its topography. However, some studies have proposed a concentration of lamellae without laterally continuous velocity discontinuity to explain complex patterns in wide-angle data (Long et al., 1994). In our case, the Moho was modelled as a 3 km wide strip centered in the digitized Moho from the refraction modelling (7.85 km/s isovelocity line). Along this strip a random lensing was performed following the same stochastic process as before. Results from these simulations provide a more reflective lower crust as a result of the constructive interference between lenses. The Moho discontinuity is imaged as a 1 second reflective band which better reproduces the real data (Figs. 5 and 6).

5. Discussion

The Moho discontinuity is clearly imaged in the six shot-gathers considered in the present work (Fig. 3). In the data acquired to the south, it appears as a simple thin weak event (shots B5 and B6) around 9.5 s in twtt. Towards the north, the Moho signature changes gradually

increasing in thickness, amplitude and complexity (shots B1, B2 and B3). To the north, this seismic event seems to be slightly deeper (10 s twtt) than in the southern edge. At large scale, the Moho can be considered as a flat interface, some prominent events in the northernmost shots of the profile may indicate a variation in its topography. Other prominent events can be identified in individual shots at lower-crustal levels but its nature as well as its real geometry is difficult to assess because of the hyperbolic time correction applied. However, these reflectors are indicative of complex structures within the base of the crust. Forward seismic modelling showed that data generated using the refraction model is able to recover the main seismic events linked to major discontinuities in the velocity model but, it is insufficient to justify complex seismic patterns observed in real data. In order to better reproduce the real seismic signature, heterogeneities must be considered. Introducing lensing/layering in mafic intrusions, lower crust and Moho, more realistic simulations are achieved where interference between small diffractor bodies (lenses) can qualitatively account for the coda observed in field shot records.

The variations in the seismic signature of lower crust and Moho as well as the changes in reflectivity patterns along the profile strongly evidence a very heterogeneous crust. Although the image lacks the quality of a continuous normal incidence stack, it is possible to distinguish different areas in the lower crust based on the differences in seismic signature. Moreover, this wide-angle transect extends to the south and east, beneath the well known Iberian Pyrite Belt, the knowledge provided by the published results for the IBERSEIS profile where the Moho appears at around 10.5 s twtt (Simancas et al., 2003; Carbonell et al., 2004). The seismic data is congruent with an idealized model that consists of strongly layered high velocity intrusions in the mid-crust, a heterogeneous lower crust and a laminated Moho, thin and simple beneath the SPZ, and thicker and more complex beneath the OMZ and CIZ (Fig. 7).

Additional work would be required to better understand the distribution of acoustic properties of the lower crust as well as the detailed structure of the Moho discontinuity for instance, adding information from S-wave data.

The wide-angle stack coupled with the synthetic modelling suggests that the crust beneath the study area features strongly laminated zones at mid-crustal depths which are characterized by relatively high velocities (Fig. 4). This zones account for the relatively high frequency reflectivity at mid-crustal depth approximately at 5 to 7 s twtt (shots B1, B4, B5 and B6) and in the wide-angle stack. The velocities and the high frequency reflectivity are consistent with layered mafic intrusions (Palomeras et al., 2009). Deemer and Hurich (1994) indicated that thin layered mafic intrusions can result in high acoustic impedances. The lower crust has been modelled as a layer with a medium degree of heterogeneity and/or lamination. This result

in a heterogeneous lower crust with lenses and/or deformed layering composed of gabbronorite to pyroxene quartz, some intrusives, gabbrodiorites intermixed with garnet granulites (Saleeby et al., 2003). These lithologies distributed in lense lense-like structures interfingering each other can account for the observed lower-crustal reflectivity.

The Moho has been modelled as consisting of a thinly laminated structure. The Moho is thicker in the center of the orogen where the reflectivity is higher and the band of reflectivity thicker. The reflection coefficients are also high towards the northern end of the transect. The Moho discontinuity also features lensing strongly develop and heterogeneous beneath the core of the orogen (the center of the transect beneath shot points B3 and B4) this lensing is most probably a mixture of lithologies that can include spinel peridotite layers interfingering garnet peridotite and gabbros (Saleeby et al., 2003; Palomeras et al., 2009).

The wide-angle stack does not constrain the upper crust, however it provides information on the mid-to-lower crust. The 1 to 2 s thick band of high reflectivity observed at the base of the crust in the wide-angle stack which can be accounted for by the models suggests that the lower crust and Moho are relatively young structures most probably developed in the late stages of the collision and a result of the crustal re-equilibration. After the collision and the strike-slip movements, during the late stages of the transpression tectonics, intense lithospheric processes were taking place, intense lower-crustal deformation, subcrustal erosion of the crustal orogenic root, most probably large amounts of upper mantle mafic melts intruded in the lower and middle crust and in some cases even up to the surface creating a unique tectonic evolution scenario which favored the development of the unprecedented large scale sulphide deposits observed at the surface. The mantle material also ponded at Moho level in the shape of thin lamelae. Thus, the signature of the terranes was not preserved with depth, rather the lower crust and Moho behave different than the upper crust during the transpression. The lower crust and Moho are most probably a result of the deformation and therefore the present day structure is a consequence of the re-equilibration processes during the late stages of the transpression. The transpression erased most of the characteristic features of the terranes and collision at lower crust and Moho depths.

Geologically, the mid-to-lower-crustal heterogeneities could be represented by elongated lenses featuring high seismic velocities. These are embedded into the mid-lower crust representing sills intrusions of mafic material which has been emplaced in weak zones within the crust (i.e., previous fractures). The synthetic seismic data produced by the model features interfingering domains of high-amplitude layered reflectivity. The seismic fabric and the high-amplitude reflectivity are consistent with layering caused by multiple
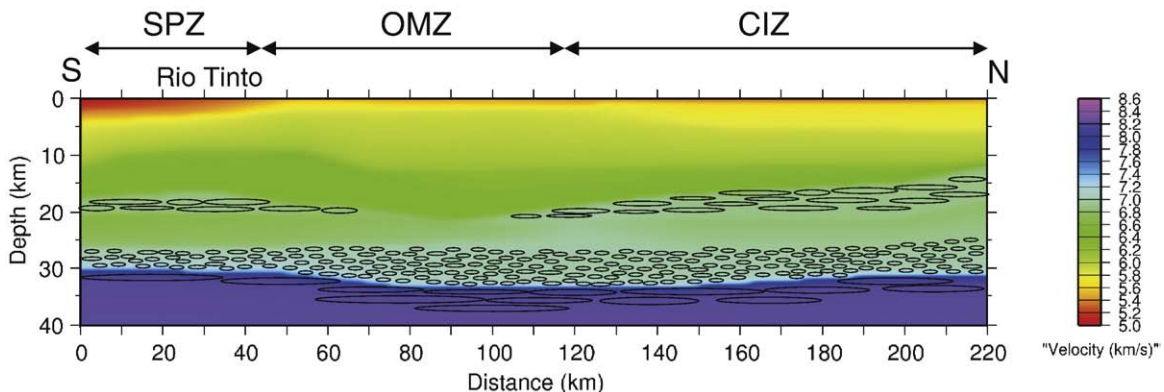

Fig. 7. Cartoon model that would account for the wide-angle data: layering/lensing in middle-crust mafic intrusions, lower crust and Moho discontinuity, across the three tectonic terranes SPZ, OMZ and CIZ.

sill lense type intrusions. The intrusion of mafic magmas in the crust assimilated part of the surrounding rocks, leaving behind relatively large amount of restites. These restites would be embedded within the lower crust resulting in more competent, higher velocity layers/lenses.

The mafic intrusion in the middle crust must have preferentially emplaced in an existing weak zones (i.e., faults, detachments). The IBERSEIS normal incidence image revealed evidences for basal detachment beneath the imbricate thrust system of the SPZ at mid-crustal depth. Which is consistent with the mid-crustal reflectivity identified in the southern end of the transect (shots B5 and B6).

Beneath the SPZ (Fig. 7) mafic layering is located at approximately 20 km depth. This layering must be simple, it most probably consist of a few relatively large sills. This structure needs to be strongly reflective because of the high-amplitude reflectivity at 7 s twtt in shots B5 and B6. Nevertheless it needs to be simple because the PMP reflection from the Moho can be identified at normal incidence offsets as a relatively thin reflection beneath this zone.

Beneath the OMZ, the band of reflectivity at the mid-to-lower crust towards the north is more transparent. Nevertheless the seismic signature of the Moho is thicker and increases slightly in depth. The thin relatively continuous PMP reflection beneath the SPZ turns into a thicker reflective band with reflection events with relatively short lateral continuity. This is qualitatively consistent with a thicker layered Moho composed of interlayering of high and low velocity lenses. This is most probably the result of the re-equilibration process, the assimilation of the root of the orogen on the OMZ which corresponds to the core of the orogen. The seismic response of the Moho discontinuity is strongly affected by the lateral dimensions of the overlying structures. These structures disperse the energy and deform the wavefront breaking up the reflection events.

Beneath the CIZ the Moho reflectivity evolves from relatively thick 0.7–1 event to a thinner and weaker event at the northern edge of the transect. This feature and the increase in reflectivity of the mid-to-lower crust have been simulated by introducing a layer of sills that increases in thickness towards the north, at 15 to 20 km in depth. This mid-crustal feature is consistent and it might represent the IRB (Iberian Reflective Body) beneath this transect. The IRB was imaged by the IBERSEIS transect which is located farther to the north-west (Fig. 1). This mid-crustal complex sill intrusion will affect the seismic signature of the Moho resulting in a weaker event.

6. Conclusions

The closely spaced wide-angle seismic dataset presented in this work, provides an image of the crust which reveals a strongly heterogeneous nature. Our results outline a picture of the Variscan lower crust as a heterogeneous media with small-scale velocity variations. Likewise, a mafic intrusion located in the middle crust features a heterogeneous layering/lensing. The full-wave forward modelling performed here shows that a simple layer cake velocity model obtained from conventional ray tracing techniques, cannot explain the lower crust reflective packages in the data. On the other hand, a qualitatively satisfactory fit of the data was accomplished when stochastic lensing was added to the refraction velocity model. This suggests that the mafic intrusion and the lower crust are strongly layered. The Moho discontinuity beneath the southern end is imaged as a thin weak reflector, accounting for a simple interface. Beneath the central part of the transect the Moho is associated to a thick high-amplitude reflective package which suggest a more complex structure. Finally, beneath the northern end, the Moho is displayed as a discontinuous interface with changing seismic signature. The wide-angle low-fold stacked section obtained from this experiment and the synthetic seismic modelling provide a new picture of the Moho discontinuity in SW-Iberia. The seismic image reveals a laterally heterogeneous Moho and a changing lower crust seismic signature along the profile. This lateral variability and the horizontality of the

lower crust and Moho suggest that they are most probably the result of the re-equilibration lithospheric processes during and after the late stages of the transpression event.

References

Blundel, D., Arndti, N., Cobbold, P., Heinrich, C., 2005. Geodynamics and ore deposits evolution in Europe. Ore Geol. Rev. 27, 1–349.

Carbonell, R., Smithson, S.B., 1991. Large-scale anisotropy within the crust in the Basin and Range province. Geology 19, 698–701.

Carbonell, R., Lecerf, D., Itzin, M., Gallart, J., Brown, D., 1998. Mapping the Moho beneath the southern Urals with wide-angle reflections. Geophys. Res. Lett. 25, 4229–4232.

Carbonell, R., Gallart, J., Pérez-Estaún, A., 2002. Modelling and imaging the Moho transition: the case of the southern Urals. Geophys. J. Int. 149, 134–148.

Carbonell, R., Simancas, F., Juhlin, C., Pous, J., Pérez-Estaún, A., González-Lodeiro, F., Muñoz, G., Heise, W., Ayarza, P., 2004. Geophysical evidence of a mantle derived intrusion in SW Iberia. Geophys. Res. Lett. 31, L11601.

Casquet, C., Galindo, C., Tornos, F., Velasco, F., Canales, A., 2001. The Aguablanca Cuni ore deposit (Extremadura, Spain), a case of synorogenic orthomagmatic mineralization: age and isotope composition of magmas (Sr,Nd)and ore (s). Ore Geol. Rev. 18, 237–250.

Christensen, N.I., Mooney, W.D., 1995. Seismic velocity structure and composition of the continental crust: a global view. J. Geophys. Res. 100, 9761–9788.

Deemer, S.J., Hurich, C.A., 1994. The reflectivity of magmatic under-plating using the layered mafic intrusion analog. Tectonophysics 232, 239–255.

Galán, G., Marcos, A., 1997. Geochemical evolution of high pressure mafic granulites from the Bacariza formation (Cabo Ortegal complex, NW Spain): an example of a heterogeneous lower crust. Geol. Rundsch. 86, 539–555.

Gibson, B.S., Levander, A.R., 1988. Lower crustal reflectivity patterns in wide-angle seismic recordings. Geophys. Res. Lett. 15, 617–620.

Holliger, K., Levander, A.R., 1992. A stochastic view of lower crustal fabric based on evidence from the Ivrea Zone. Geophys. Res. Lett. 19, 1153–1156.

Holliger, K., Levander, A.R., Goff, J.A., 1993. Stochastic modeling of the reflective lower crust: petrophysical and geological evidence from the Ivrea Zone (northern Italy). J. Geophys. Res. 98, 11.967–11.980.

Holliger, K., Levander, A., Carbonell, R., Hobbs, R., 1994. Some attributes of wavefields scattered from Ivrea-type lower crust. Tectonophysics 232, 267–279.

Hurich, C.A., Smithson, S.B., 1987. Compositional variation and the origin of deep crustal reflections. Earth Planet. Sci. Lett. 85, 416–426.

Levander, A., England, R.W., Smith, S.K., Hobbs, R.W., Goff, J.A., Holliger, K., 1994a. Stochastic characterization and seismic response of upper and middle crustal rocks based on the Lewisian gneiss complex, Scotland. Geophys. J. Int. 119, 243–259.

Levander, A., Hobbs, R.W., Smith, S.K., England, R.W., Snyder, D.B., Holliger, K., 1994b. The crust as a heterogeneous "optical" medium, or "cocodriles in the mist". Tectonophysics 232, 281–297.

Long, R.E., Matthews, P.A., Graham, D.P., 1994. The nature of crustal boundaries: combined interpretation of wide-angle and normal-incidence seismic data. Tectonophysics 232, 309–318.

Martínez-Catalán, J.R., Arenas, R., Díaz-García, F., Abati, J., 1997. The Variscan accretionary complex of NW Iberia: involved terranes and successions of tectonothermal events. Geology 25, 1103–1106.

Martini, F., Bean, C.J., Dolan, S., Marsan, D., 2001. Seismic image quality beneath strongly scattering structures and implications for lower crustal imaging: numerical simulations. Geophys. J. Int. 145, 423–435.

Palomeras, I., Carbonell, R., Flecha, I., Simancas, F., Ayarza, P., Matas, J., Martínez Poyatos, D., Azor, A., González Lodeiro, F., Pérez-Estaún, A., 2009. Nature of the lithosphere across the Variscan Orogen of SW Iberia: Dense wide-angle seismic reflection data. J. Geophys. Res. 114, B02302.

Peucat, J.J., Bernard-Griffiths, J., Gil-Ibarguchi, J.I., Dallmeyer, R.D., Menot, R.P., Cornichet, J., de Leon, M.I.-P., 1990. Geochemical and geochronological cross section of the deep Variscan crust; the Cabo Ortegla high-pressure nappe (northwestern Spain). Tectonophysics 177, 263–292.

Ribeiro, A., Sanderson, D., Colleagues, S.I., 1996. EUROPROBE 1996 — lithosphere dynamics: origin and evolution of continents, chapter SW-Iberia. Transpressional Orogeny in the Variscides. Uppsala University, pp. 91–95.

Rutter, E.H., Khazanehdari, J., Brodie, K.H., Blundell, D.J., Waltham, D.A., 1999. Synthetic seismic reflection profile through the Ivrea Zone-Serie dei Laghi continental crustal section, northwestern italy. Geology 27, 79–82.

Saleeby, J., Ducea, M., Clemens-Knott, D., 2003. Production and loss of high-density batholitic root, southern Sierra Nevada, California. Tectonics 22, 3(1)–3(24).

Santos-Zalduegui, J.F., Schrarer, Y., Gil-Ibarguchi, J.I., Girardeau, J.J., 1997. Origin and evolution of the Paleozoic Cabo Ortegal ultramafic–mafic complex (NW-Spain). Chem. Geol. 129, 281–304.

Simancas, F., Martínez-Poyatos, D., Expósito, I., azor, A., González-Lodeiro, F., 2001. The structure of a major suture zone in the SW Iberian massif: the Ossa-Morena/Central-Iberian contact. Tectonophysics 332, 295–308.

Simancas, J.F., Carbonell, R., González-Lodeiro, F., Pérez-Estaún, A., Juhlin, C., Ayarza, P., Kashubin, A., Azor, A., Martínez-Poyatos, D., Almodóvar, G.R., Pascual, E., Sáez, R., Expósito, I., 2003. Crustal structure of the transpressional Variscan orogen of SW Iberia: SW Iberia deep seismic reflection profile (IBERSEIS). Tectonics 22, (1)-1–(1)-20.

Sochacki, J.S., Kubichek, R., George, J.H., Fletcher, W.R., Smithson, S.B., 1987. Absorbing boundary conditions and surface waves. Geophysics 52, 60–71.

Sochacki, J.S., George, J.H., Ewing, R.E., Smithson, S.B., 1991. Interface conditions for acoustic and elastic wave propagation. Geophysics 56, 168–181.

Tornos, F., Casquet, C., Galindo, C., Velasco, F., Canales, A., 2001. A new style of Ni-Cu mineralization related to magmatic breccia pipes in a transpressional magmatic arc, Aguablanca, Spain. Miner. Depos. 36, 700–706.

Wenzel, F., Sandmeier, K.-J., Wälde, W., 1987. Properties of the lower crust from modeling refraction and reflection data. J. Geophys. Res. 92, 11.575–11.583.